Proceedings of the 17th World Congress
The International Federation of Automatic Control
Seoul, Korea, July 6-11, 2008

Advanced Control Techniques for Semiconductor and Flat Panel Display Substrate Handling Robots

Martin Hosek* Jairo T. Moura**

Brooks Automation, Inc., Chelmsford, MA 01824, USA
**E-mail: martin.hosek@brooks.com*
***E-mail: jairo.moura@brooks.com*

Abstract: Substrate-handling robots for semiconductor and flat-panel-display manufacturing applications possess undesirable structural flexibilities and frictional effects which erode closed-loop stability and deteriorate tracking performance. In this study, advanced control and identification techniques are applied to cope with these control challenges. The techniques include sensorless modal stabilization, observer-corrector control strategy, iterative learning control approach and neural-network-based perturbation estimation. The fundamentals of the techniques are reviewed and the resulting performance improvements are demonstrated experimentally.

1. INTRODUCTION

The existing manufacturing technologies for semiconductor integrated circuits and flat panel displays include processing of silicon wafers and glass panels, referred to as substrates, in fully automated vacuum cluster tools, which are serviced by one or more robots (Caveney and Hofmeister 1998, Davis and Brooks 1988, Hendrickson 1993, Davis and Hofmeister 1997). Typical operations performed by the robots include elementary rotational and straight-line moves, which are often combined and blended into more complicated planar or three-dimensional trajectories in order to comply with complex workspace geometries (Hosek and Elmali 2001, 2003).

Increasing complexity, strict space constraints and limited weight of moving components required for high-speed performance and low power consumption lead to compromised structural stiffness of the robots. As a result, the rigid body dynamics of the robots is often accompanied by a number of position-dependent lightly-damped vibration modes (resonance conditions) which interfere with traditional control techniques developed for rigid robots, causing undesirable oscillations, affecting overall stability, and leading to limited control performance. Implementation of low-pass filters and band-reject filters, an approach often adopted in the engineering practice to cope with structural resonances, is not effective for high-performance robots since low-pass filters introduce amplitude distortion and destabilizing phase lag, which deteriorates control performance, and band-reject filters are not suitable for applications where the resonance conditions shift during operation, change due to regular wear and tear, or vary because of production inconsistency. Therefore, alternative control methods, which do not increase the hardware complexity (no additional sensors and actuators) and do not demand excessive computational capacity, are needed for high-performance industrial applications.

The robots typically hold the substrate subject to processing by means of a vacuum-operated suction-type or edge-contact gripper. In order for the vacuum lines to pass through revolute joints with unlimited rotation, such as in the case of the wrist joints of robot arms with articulated end-effectors, the joints incorporate a system of passages with seals between the rotating components of the joints. Similarly, electrical signals for substrate sensors and scanners (mappers) mounted on the robot end-effectors are routed through the robot joints using multiple slip-rings. The seals and slip-rings introduce undesirable friction. Additional sources of friction, dry and viscous, are associated with pre-loaded bearings of the robot arm. The frictional effects negatively affect tracking and settling performance of the robot.

This paper presents an overview of innovative methods developed and/or applied by the authors to address the above control challenges. In Sections 2 and 3, two control concepts, sensorless modal stabilization and observer-corrector control, are utilized to reduce undesirable effects of resonance conditions. In Sections 4 and 5, additional two techniques, iterative learning control approach and neural-network-based perturbation estimation, are applied to cope with undesirable frictional effects. The fundamentals of each of the methods are reviewed and the resulting performance improvements are demonstrated experimentally.

2. SENSORLESS MODAL STABILIZATION

A control approach based on sensorless modal stabilization (Hosek 2001a) is a method suitable for robots where undesirable structural flexibilities introduce vibration modes *within* the required bandwidth of operation of the motion controller, resulting in destabilization of the closed-loop system. In contrast to conventional methods where the frequency components corresponding to the undesirable vibration modes are filtered out in the control loop (e.g. Friedland 1996, Levine 1996a), the key idea in this approach is to use a composite controller which consists of a trajectory-tracking section for the rigid-body dynamics complemented by a vibration-damping compensator for the flexible dynamics of the robot. The vibration damping compensator requires information on the states of the dominant flexible dynamics. Since direct measurements of these states are not available in a majority of applications, they need to be replaced by approximate estimates. A reduced-order state observer is employed for this purpose.

As an example, the control method is applied to a three-link SCARA-type MagnaTran 77 robot for flat-panel-display manufacturing applications (inset in Fig. 1). While the first two links of the robot, the upper arm and forearm, are driven

independently by a pair of motors, a belt arrangement is employed to maintain radial orientation of the end-effector regardless of the position of the first two links. The inevitable elasticity of the belt arrangement introduces a problematic vibration mode, the frequency of which varies substantially with the radial extension of the arm (Fig. 2a).

A simplified block diagram of the composite controller is presented in Fig. 1. The trajectory-tracking controller and vibration-damping compensator are referred to as motion controller and stabilizing controller, respectively, in the figure. The following nomenclature is adopted: 'R' and 'T' represent the commanded (reference) trajectory in terms of the polar coordinates of the end-effector, 'θ_{r1}' and 'θ_{r2}' denote the commanded trajectory converted to angular positions of the motors, 'τ_1' and 'τ_2' are torques exerted by the motors, 'θ_1' and 'θ_2' stand for angular positions obtained from the motor encoders, and 'e' denotes angular displacement of the end-effector from its equilibrium position.

The trajectory-tracking controller operates based on position and velocity feedback using a standard implementation of the computed torque technique (e.g. Fu et al. 1987). It comprises a rigid-body model of the robotic manipulator complemented by a PD compensator with a disturbance observer for each of the motors (a disturbance observer is used in place of a conventional I-control for improved tracking and prompt elimination of steady state errors).

The purpose of the vibration-damping compensator is to enhance damping characteristics of the dominant flexible dynamics, in this particular case associated with the elastic belt arrangement, improving overall stability properties of the system. The compensator design is based on the state formulation of the linearized robot dynamics. It is selected in the form of state feedback from the displacement and velocity of the robot end-effector (PD control). The control gains are determined using a pole-placement technique complemented by LQR optimization to obtain a unique solution. They are selected so that the closed-loop system, i.e., the robot with the composite controller, is stable in the required workspace.

The vibration-damping compensator requires information on the states of the flexible dynamics which is subject to control, in this particular case the dynamics of the end-effector of the robotic arm. Since direct measurements of these states are not available in practice, they need to be replaced by approximate estimates. A reduced-order state observer is employed for this purpose. The state estimation is based on an approximate theoretical model of the robotic manipulator. The observer is designed with a limited bandwidth selected so that it satisfactorily tracks the dynamics of interest but does not respond to higher-frequency inputs associated with unmodeled dynamics and measurement noise.

The state observer and vibration-damping compensator can be employed only when the flexible dynamics subject to control is observable and controllable. In order for the robotic manipulator to operate in its entire workspace, a mechanism is implemented which allows the arm to move through or hold in positions where the flexible dynamics is unobservable and uncontrollable. In this particular application, the unobservable and uncontrollable positions coincide. Consequently, the state observer and vibration-damping compensator can be turned off in the neighborhood of the unobservable and uncontrollable positions, and activated again when the robot moves outside of this zone. In order to avoid initial step change in the observer output, which may result from the inputs being non-zero at the time of activation of the observer, the state vector of the observer must be initialized so that the desired initial observer output is obtained. Activation of the vibration-damping compensator is delayed with respect to the state observer in order to allow the initial transient of the observer output to decay. This mechanism guarantees smooth transition to full operation of the vibration-damping compensator.

The stabilizing effects of the vibration-damping controller are demonstrated in terms of the response of the closed-loop system to nonzero initial conditions imposed on the flexible dynamics associated with the elastic belt. The tip of the end-effector of the arm is displaced from its equilibrium position while the robot is commanded to stay in a specified radial position. The displacement of the end-effector induces errors in the positions of the robot encoders which are eventually eliminated by the disturbance observers, resulting in deformation of the belt. The end-effector is released at this point. Fig. 2b indicates instability of the closed-loop system when the vibration-damping compensator is not used (eventually, a limit cycle is reached since the motor torques are limited). Substantial stability improvements are observed with the vibration-damping controller activated.

The tracking performance of the composite control system is tested for a simple straight-line move in the radial direction. A comparison of the control performance with and without the vibration-damping controller is presented in Fig. 3. The graphs indicate that the stability and, consequently, the tracking performance of the robotic manipulator improve considerably when the vibration-damping compensator is implemented.

In summary, the practical contribution of the sensorless modal stabilization concept consists in improved stability and control performance. These improvements are achieved with no additional sensory and/or actuation arrangements that would lead to undesirable increase of hardware complexity. Detailed information on the controller design and state observer implementation, including a complete test report, is provided in Hosek (2001a).

3. OBSERVER-CORRECTOR CONTROL

The observer-corrector control strategy (Hosek 2001b; Hosek et al. 2001, 2003) has been developed for applications where undesirable resonance conditions appear at frequencies *above* the minimum bandwidth necessary for required operation of the robot. In this approach, the system subject to control is viewed in terms of its dominant dynamics, which is essential to achieve required functionality, and the resonance properties associated with higher-order dynamic effects, which are imposed on the dominant dynamics and considered to be unnecessary and undesirable for proper operation. The objective is to extract the dominant dynamics essential for operation of the robot with minimal amplitude and phase distortion of feedback signals. For this purpose, a substitute feedback signal is synthesized using a unique arrangement of a band-limited state observer and a low-pass filter corrector. The synthetic signal is then used as a controller input, effectively reducing destabilizing effects of unmodeled dynamics of the robot.

A conceptual block diagram of the observer-corrector arrangement is depicted in Fig. 4, where 'r' denotes the reference signal, 'e' is the control error, 'u' refers to the control action, 'd' is external disturbance, 'n' stands for measurement noise, 'y' is the output of the robot, 'y_o' represents the output of the state observer, 'y_c' is the output of the corrector filter, and 'y_s' is the synthetic feedback signal. The symbols may represent

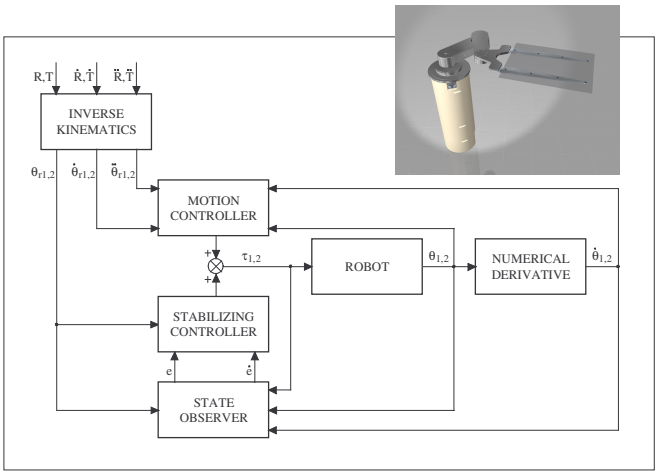

Fig. 1. Block diagram of composite control system; test MagnaTran 77 robot (inset).

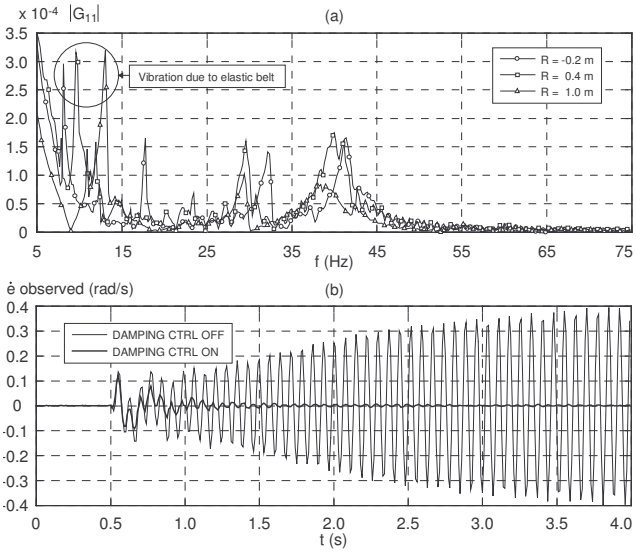

Fig. 2. Composite control - (a) frequency response of test robot, (b) response to nonzero initial conditions.

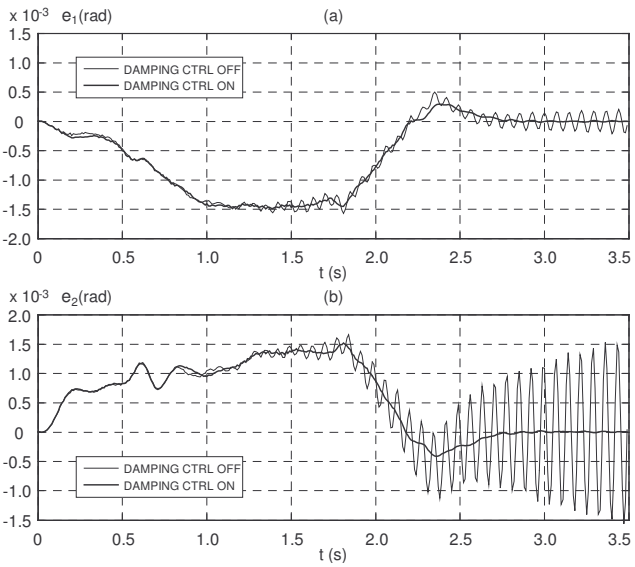

Fig. 3. Composite control - tracking errors, (a) motor 1, (b) motor 2.

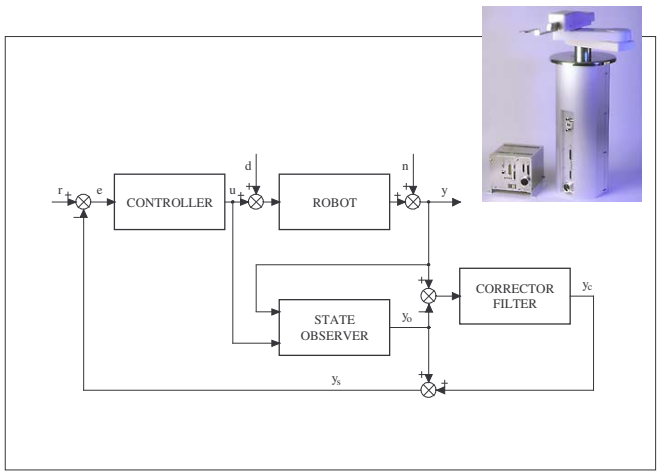

Fig. 4. Block diagram of observer-corrector control system; test AquaTran 7 robot (inset).

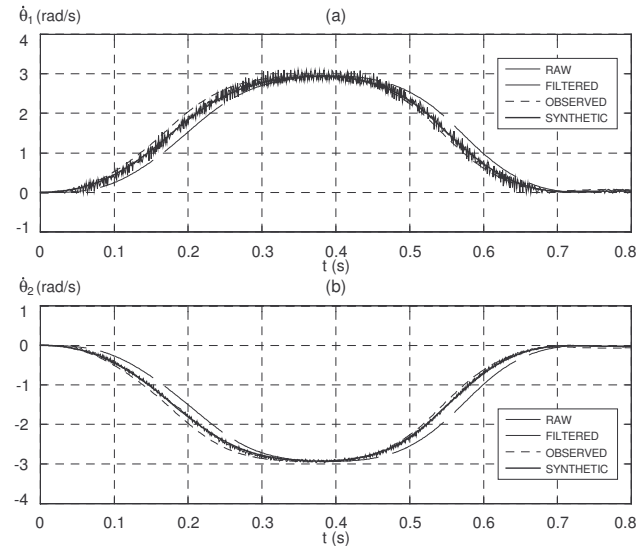

Fig. 5. Observer-corrector control - velocity profiles, (a) motor 1, (b) motor 2.

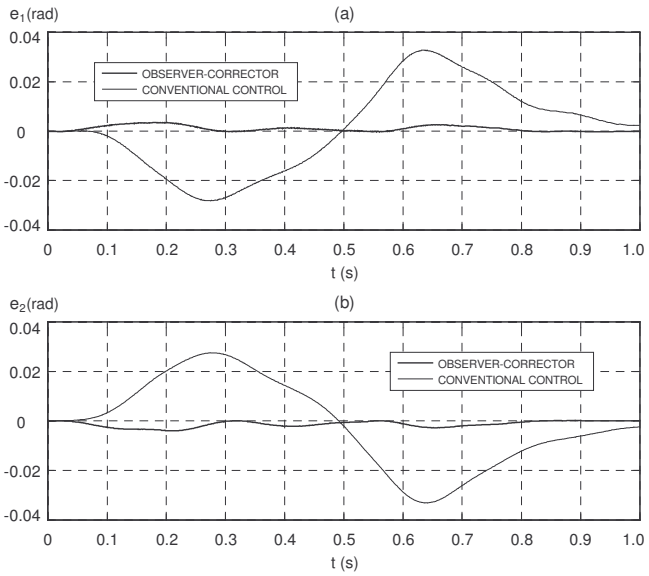

Fig. 6. Observer-corrector control - tracking errors, (a) motor 1, (b) motor 2.

either scalar variables or vectors, depending on the number of axes of the robot.

It is assumed that the undesirable resonance conditions of the robot (i.e., higher-order dynamic effects) appear at frequencies above the bandwidth essential for required operation (i.e., dominant dynamics). This allows for the dominant dynamics and the undesirable higher-order dynamic effects to be separated in the frequency domain. The external disturbance is expected to be relatively slow, i.e., of low-frequency contents, in comparison with the higher-order dynamics of the robot. The measurement noise is assumed to be of high-frequency nature compared to the bandwidth of the dominant dynamics. These assumptions are realistic for typical robot control applications. They reflect the requirement that the bandwidth of the dominant dynamics of the robot and the disturbance to be compensated for cannot overlap with the frequency contents of the measurement noise in order for the control to be effective. In accordance with these assumptions, the output of the robot can be decomposed into two parts: a component which reflects the dominant dynamics, and a component which corresponds to the higher-order dynamics and noise.

Referring still to Fig. 4, the state observer is employed for on-line estimation of the state and output variables associated with the dominant dynamics of the robot. It is designed with a limited bandwidth selected so that it satisfactorily tracks the dominant dynamics of the robot but does not respond to the higher-frequency inputs which are associated with the higher-order dynamics and measurement noise. The accuracy of the estimated output of the robot is limited due to observation errors which typically result from modeling imperfections and, as such, are of low-frequency nature.

In order to compensate for the mismatch between the output of the state observer and the actual dominant dynamics of the robot, the corrector filter is incorporated into the control system, as suggested in Fig. 4. It is selected as a linear low-pass filter to let through the lower-frequency components corresponding to the dominant dynamics and observation errors, and attenuate the higher-frequency components of the undesirable dynamics and measurement noise. The input of the corrector filter is calculated as a difference between the output of the robot and the estimate obtained from the state observer. As a result, the components of the dominant dynamics of the robot are effectively removed from the input of the corrector filter. Since the corrector filter is designed to attenuate the undesirable frequency components corresponding to the higher-order dynamics and noise, its output reduces approximately to the negative of the state observer estimation error.

Finally, the estimated output of the robot obtained from the state observer, y_o, and the output of the corrector filter, y_c, are combined to synthesize the substitute feedback signal, y_s. At this point, the state observer estimation error approximately cancels with its negative from the output of the corrector filter, producing a synthetic signal which is equivalent to the dominant dynamic component in the output of the robot.

The resulting synthetic signal can be viewed as an output of a virtual robot which assumes the dominant dynamics of the actual system, but does not exhibit the undesirable higher-order dynamic effects. Consequently, the controller can be designed practically without taking the higher-order dynamic effects into account, which allows for use of conventional control techniques, and translates into reduced modeling requirements, simplified controller design and shorter development time when compared to a complete dynamic analysis.

The performance of the observer-corrector control strategy is tested on a direct-drive wafer-handling robot AquaTran 7 for atmospheric and corrosive environments (inset in Fig. 4). The robot performs a radial straight-line move. The effects of the observer-corrector arrangement in the velocity control loop are shown in Fig. 5, where indices 1 and 2 refer to the motors which drive the upper arm and forearm, respectively. The raw velocity signals are visibly contaminated by undesirable high-frequency components (hairline). Conventionally, they would be passed through low-pass filters, resulting in significant phase-lag distortion (dashed line), and fed back to the controller. In the observer-corrector strategy, in contrast, the feedback signals originate in the state observer (dotted line), and the low-pass filters are employed merely to correct inevitable observation errors resulting from modeling imperfections. Combining the observed velocities with the outputs of the corrective filters yields clean synthetic signals which closely follow the raw velocities but do not contain undesirable high-frequency components (bold line). The signals show substantially smaller errors than the filtered and observed velocities alone.

In order to quantify the improvement achieved due to the observer-corrector mechanism, the control performance is compared with an equivalent conventional control approach in terms of motor tracking errors. The state observer is disconnected in this case. The raw velocity signals are passed through low-pass filters and fed back to the controller. The control parameters remain the same except for the bandwidth, which must be reduced in order to preserve stability and non-oscillatory behavior of the system. The tracking errors are compared in Fig. 6. The graphs indicate that the tracking performance of the conventional control (hairline) is improved by an order of magnitude by implementing the observer-corrector mechanism (bold line).

The test results demonstrate significant improvements of the control performance in terms of tracking errors despite the presence of numerous position-dependent lightly-damped vibration modes. In comparison with conventional low-pass filtering, which is often adopted in practice to cope with structural resonances, the observer-corrector arrangement attenuates frequency components corresponding to the destabilizing higher-order dynamics without introducing significant amplitude distortion and destabilizing phase lag within the bandwidth of operation. Since this attenuation is not selective, the strategy is robust against changes in resonance frequencies, as long as they remain above the limit for which the observer-corrector arrangement is designed. These frequency shifts occur due to position dependency of the vibration modes and changing load conditions of the robotic manipulator, because of regular tear and wear, and result from inevitable differences between robots due to manufacturing inconsistency.

A detailed description of the observer-corrector control strategy, including a complete report on the test implementation, can be found in Hosek (2001b) and Hosek et al. (2001). The strategy is subject to a patent protection (Hosek et al. 2003).

4. ITERATIVE LEARNING CONTROL

A technique applicable to robots which exhibit various frictional effects and other difficult-to-model phenomena is iterative learning control (ILC) (e.g. Bien and Xu 1998). This approach requires repetitive behavior of the dynamics of the system and, therefore, is suitable for those substrate-handling applications where the nature of the robot motion is repetitive, i.e., the robot performs identical operations utilizing predefined trajectories that do not change. This is often true in cluster tool applications

where the robot performs pick and place operations within a given set of stations. In this case, each motion starts from an a priori known position and ends at another previously known destination.

The above described application fits in the class of ILC because (Bien and Xu 1998): (1) Every substrate transfer motion ends in a fixed time of duration; (2) A desired output trajectory is known a priori over that time of duration; (3) Repetition of the initial state is always satisfied; (4) Invariance of the system dynamics is ensured throughout the repeated moves; (5) The output error can be used in the construction of the control input for the next move; (6) There is a unique control input that yields the desired output trajectory.

If the control application fits the characteristics (1) to (6) above then the problem is to find a recursive control law that makes the output error converge to zero as the number of motion iterations increases. Each iteration consists of the motion needed to transfer the substrate from one given station to another given station. The control signal for the next substrate transfer can be computed based on the output error and control of the previous transfer.

In the present application, the ILC is proposed to enhance performance of an existing computed-torque controller, as shown in Fig. 7. In the computed-torque method (e.g. Fu et al. 1987), the control law can be viewed in terms of two fundamental parts: a model-based portion complemented by an error-driven compensator. The model-based portion employs the dynamic model of the robotic manipulator to linearize and decouple the rigid-body dynamics of the robot so that it can be represented by a pair of independent unit inertia moments associated with the motors subject to control.

The performance of the computed-torque motion control algorithm is limited by the accuracy of the dynamic model and the bandwidth of the error-driven compensator. In order to meet performance specifications (e.g., position tracking), the control engineer needs to complete the following two steps: (1) Build the dynamic model, often based on measured parameters; (2) Tune the controller bandwidth, hoping that the performance specifications can be met without undesirable excitation of flexible dynamics (structural resonances).

The ILC is utilized to complement the dynamic model to compensate for unmodeled effects, such as dry friction, viscous damping, parameter uncertainties and other difficult-to-model phenomena, thus improving the performance and reducing the contribution of the error-driven compensator. As a result, the compensator can operate with a lower bandwidth, which reduces the risk of excitation of the flexible dynamics.

The unmodeled effects manifest themselves as disturbances. A disturbance signal can be defined by a measure of the discrepancy between the actual dynamics and the theoretical dynamic model. One way to quantify this signal is to compare the actual and predicted accelerations of individual joints of the robot as explained in Elmali and Olgac (1992) and Moura et al. (1997). This definition is adopted in the present study.

The actual disturbance is unknown in real time. If the disturbance were known, exact information on the robot dynamics would be available and, consequently, the robot would be able to track the desired trajectory perfectly without any contribution of the error-driven compensator. In other words, if the dynamics of the robot became perfectly known, no closed loop component would be needed in order to track a prescribed motion trajectory.

The fact that the actual disturbance is not known in real time does not mean that it cannot become available after the motion has finished. This observation is of extreme importance for a system that is *repetitive*. As explained earlier, substrate transfer operations are often repetitive tasks. Therefore, it is possible to identify the actual disturbances for a given substrate transfer operation and utilize this information to substantially reduce the tracking errors without the need for changing the bandwidth of the error-driven compensator or adjusting the dynamic model parameters.

The fundamental idea of the proposed implementation of ILC consists of two basic steps: (1) Recording of the actual disturbance during a given motion iteration; (2) Playing the learned disturbance in the next motion iteration (Fig. 7).

The process of recording consists in storing the disturbance signal for all the joints in a vector that can be reproduced or played at any time after the motion has finished. In the next move iteration, the previously recorded disturbance can be used in the control law as a correction for the modeling errors. When this is done then the recorded vector is no longer a disturbance for the current motion since it became known to the controller. In other words, the controller learned the unknown disturbance.

An efficient way of storing the disturbance signals is in terms of their FFT coefficients. Conveniently, by truncating the series of the FFT coefficients, the frequency spectrum of the disturbance signals can be bounded within a desired range, thus eliminating unwanted higher frequency noise.

The actual disturbance cannot be assimilated in a single iteration due to the presence of non-repetitive external perturbations. The learning algorithm has to be designed such that only the repetitive disturbances are recorded and learned. This presents some robustness issues associated with the learning process. However, the learning rate can be tuned so that the controller can gradually assimilate meaningful disturbances without divergence of the learning process and, more importantly, keeping the global closed loop stability.

Fig. 8a illustrates one disturbance learning iteration for a radial extension move of a SCARA-type AcuTran 3 prototype robot of Fig. 7. The thin line is the learned disturbance signal from the previous move. The other signal (bold line) represents the non-learned portion of the disturbance during the next move, referred to as residual disturbance in the figure. The key point here is to show that the magnitude of the actual disturbances was substantially reduced in the next move iteration (residual disturbance). This means that the discrepancy between the predicted dynamics (dynamic model and learned disturbance) and the real robot dynamics was dramatically decreased, i.e., the control system learned more about the modeling errors. This is possible since the disturbance is recorded in one move iteration and feed-forwarded to the controller in the following iteration. This learning process can continue through a series of move iterations until all disturbance signals are completely assimilated (or learned) by the control law. Note that the learned signal does not have high frequency components as in the actual signal. This is another desirable feature of the proposed algorithm, i.e., it only learns meaningful frequency components since it can truncate the entire spectrum above a prescribed threshold.

Fig. 8b shows the practical effect of the learning process in terms of the position tracking errors for a radial extension move. The tracking errors are measured in the direction normal to the commanded path of the robot end-effector. As it can be seen, after the learning process takes place (bold line), the peak

normal error is reduced from the initial value of 1130 μm down to 94 μm.

In order to illustrate the stability of the learning process, a series of radial extend and retract moves was performed to/from the same radial location, and the peak tangential error was recorded for each move iteration. Fig. 9 shows the peak errors of a series of over one thousand of extend and retract moves. The "learning phase" can be seen in the first 20 moves, which exhibit substantial decrease of the peak tracking errors. After that, the learning process reaches a "steady state". The "learning limit" is achieved when there remain no repeatable components to learn.

A limitation of the ILC approach is the fact that it applies to a specific move of the robot. That is, after the learning phase is completed, the performance is optimized for that specific move utilized in the learning phase. Any changes related to the learning trajectory require additional learning. This makes this approach impractical for applications where robot station coordinates change between the time the robot was shipped from the factory to the time it is finally operating in the cluster tool, and for applications where trajectories change during operation, such as when performing offset pick operations from a substrate aligner or place operations with correction offset in systems equipped with on-the-fly substrate eccentricity recognition (Hosek and Prochazka 2005).

5. NN-BASED PERTURBATION ESTIMATION

The limitations of the ILC approach can be avoided by utilizing a neural network (NN) for estimation of modeling errors and compensation for their effects. This is because a neural network is able to predict the behavior of a non-linear function provided that its inputs lie anywhere within the training grid (e.g. Rojas 1996).

The key element of the proposed method (Moura and Hosek 2003) is a neural network incorporated into the motion controller as an additional feed-forward component which complements the computed-torque scheme, as shown in Fig. 10. The following nomenclature is used in the figure: 'θ_r' is vector of reference positions, 'θ' is vector of actual positions, 'u' is vector of control signals, 'u_C' is output of the feedback compensator, 'u_{DM}' is output of the dynamic model, 'u_{NN}' is output of the neural network, and 'M' denotes inertia matrix of the dynamic model. In vectors θ, θ_r, u, u_C, u_{DM} and u_{NN}, each element corresponds to one axis of the robot.

The purpose of the neural network is to compensate for effects of dry friction, viscous damping, parameter uncertainties and other unmodeled components, referred to as model perturbations. In addition to compensation for model perturbations, the present application requires the method to meet the following objectives: (1) To be compatible with a motion controller based on the computed-torque technique; (2) To preserve the stability properties of the computed-torque motion controller.

It is assumed that the model perturbations are functions of the joint positions, velocities and accelerations. Consequently, these variables are selected as the inputs for the neural network. The outputs of the network produce the unmodeled feed-forward portions of the control signals. The network is designed to include two layers, an input layer and an output layer. The input layer consists of a set of tangent-sigmoid neurons. The output layer comprises a pair of linear neurons. Each output of the neural network corresponds to feed-forward signal for one axis. The tangent sigmoid functions are selected for the input layer because they can model accurately non-linear functions with a finite number of discontinuities. The linear functions are chosen for the output layer in order to scale the range of the outputs.

In the proposed approach, the neural network is trained incrementally to reproduce the unmodeled portion of the control signal based on batches of data recorded over given periods of time. In the initial training step, the network learns the output of the feedback compensator, u_C. Once the initial training step has been completed, the resulting weights (NN parameters) are implemented, leading to reduction of the control signal produced by the feedback compensator. In the subsequent training steps, the network learns the remaining unmodeled components of the control signal, i.e., u_{NN}^{k+1} should match $u_C^k + u_{NN}^k$, where k indicates the training step. Ideally, for a given $k > L$ (L is finite) the output of the feedback compensator will be virtually zero since the neural network is already outputting the necessary control signal.

The neural network is trained off-line using the Levenberg-Marquard algorithm (e.g. Levine 1996b). This algorithm is selected due to its fast convergence properties. A disadvantage of this method is that it requires the inverse of a large matrix. However, tests have proven that a LU decomposition method (e.g. Press et al. 1990) is adequate for the present application. The batch data are collected in real time using a sequence of training moves, also referred to as a training grid.

It should be noted that, in the proposed arrangement, the original computed-torque motion controller, comprising a feedback compensator and a dynamic-model-based feed-forward mechanism, remains intact. This is important to achieve acceptable performance of the robot during initial training of the neural network. As mentioned earlier, the inputs of the neural network are selected to be joint positions, velocities and accelerations. In order to preserve the stability of the original computed-torque method, the reference inputs are used instead of the measured ones.

The proposed method is applied to the motion control of a five-axis direct-drive Reliance 8 robot (inset in Fig. 10), used for substrate-handling operations in semiconductor manufacturing applications. The robot holds the substrates subject to processing by means of a vacuum-operated suction-type or edge-contact gripper. In order for the vacuum lines to pass through revolute joints with unlimited rotation (e.g., the wrist joints associated with the two articulated end-effectors), the joints incorporate a system of passages with seals between the rotating components of the joints. Additionally, electrical signals for substrate sensors and scanners (mappers) mounted on the robot end-effectors are routed through the joints using multiple slip-rings. The seals and slip-rings introduce undesirable friction, which complements usual frictional effects associated with pre-loaded bearings of the robot arm.

The control system of the test robot is of distributed type. It comprises a pair of controllers that are referred to as main and remote. The main controller is in charge of overall trajectory planning, and performs feedback control of the motors which drive the first two links. The remote controller is installed inside of the robot arm to control the end-effector motors, thus reducing the number and length of signal lines that need to be fed through the links and joints of the arm. The two controllers are connected through a communication line that is used for transmission of trajectory information, but cannot be utilized to share run-time data due to limited speed and reliability-related concerns.

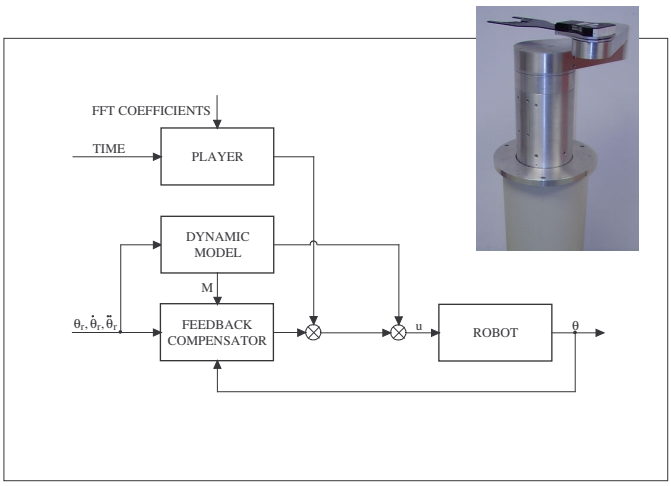

Fig. 7. Block diagram of iterative learning control; test AcuTran 3 robot (inset).

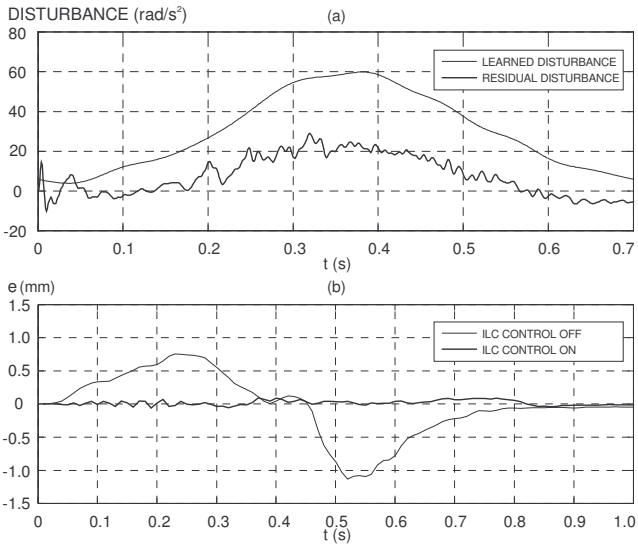

Fig. 8. Iterative learning control - (a) learned and residual disturbances after one iteration, (b) normal tracking errors.

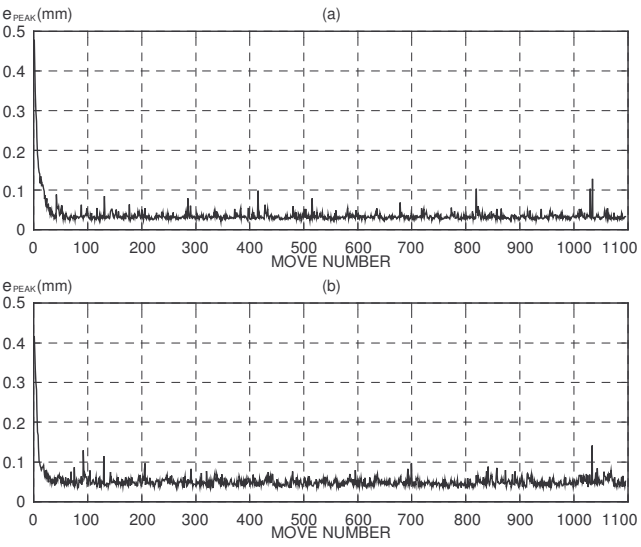

Fig. 9. Iterative learning control - peak tracking errors, (a) extend motion, (b) retract motion.

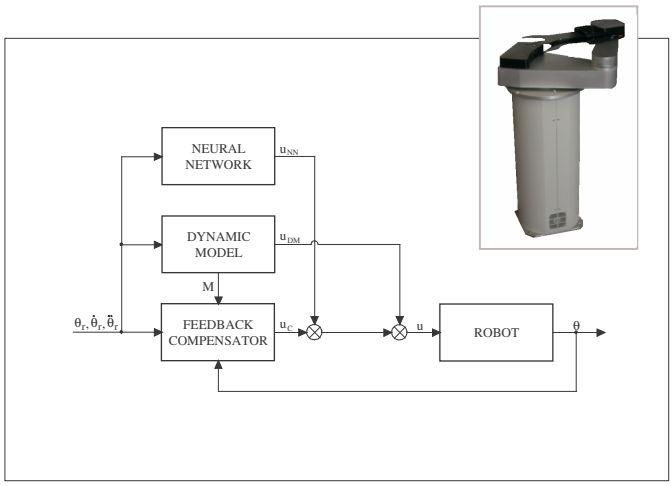

Fig. 10. Block diagram of control with NN-based perturbation estimation; test Reliance 8 robot (inset).

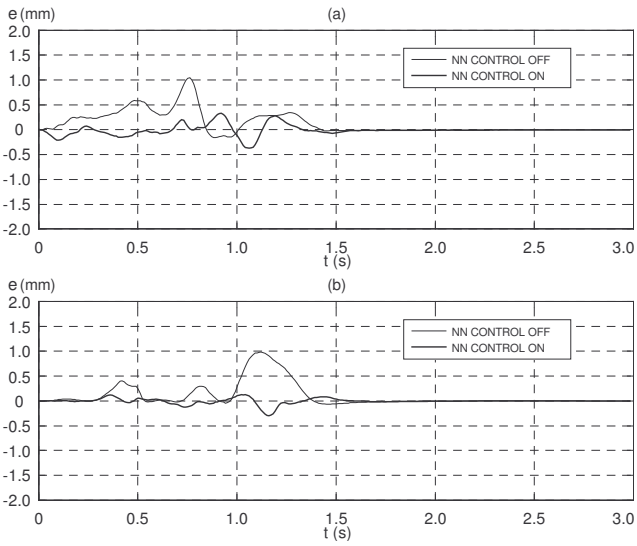

Fig. 11. NN-based perturbation estimation - normal tracking errors for 1st station, (a) extend motion, (b) retract motion.

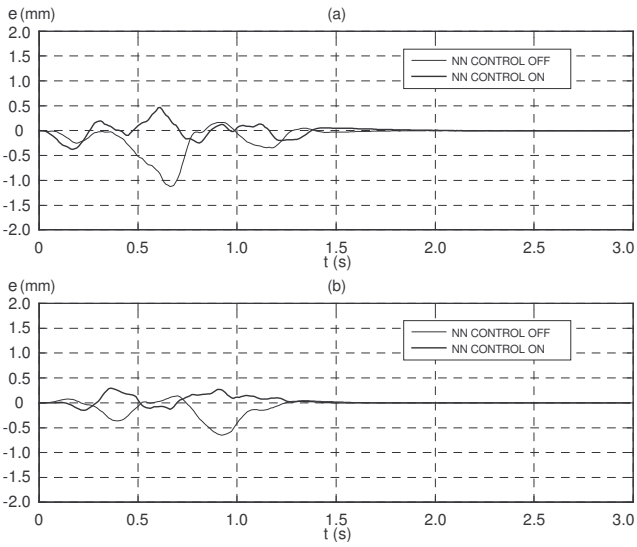

Fig. 12. NN-based perturbation estimation - normal tracking errors for 2nd station, (a) extend motion, (b) retract motion.

The robot is challenging to control, particularly due to: (1) High friction coupling between the upper and lower end-effectors; (2) The distributed control architecture, which does not allow the controllers to have real time access to all the states in all the joints; due to this limitation it is not possible to utilize an accurate model of the dynamic coupling between all joints. The limitations above have driven the proposed design of the NN-based control.

In the present application, two neural networks are implemented: one in the main controller and the other in the remote controller. Each network output is trained to provide the necessary feed-forward control signal to drive the respective robot joints as close as possible to their commanded (reference) trajectories. The inputs for both networks are identical. For the main controller, the outputs correspond to the joint torques of the first two links. For the remote controller, the outputs are defined as the torques for the two end-effectors.

In typical operation, the robot is frequently commanded to track a trajectory referred to as a via move. The selected (or active) end-effector extends and retracts along two line segments, which are blended into a smooth path around a common via-point, while the other (trailing) end-effector moves simultaneously in such a way that its orientation always points toward the shoulder joint of the robot (Hosek and Elmali 2003). Two operations of this type, each utilizing a distinct path in a different area of the robot workspace, are selected for experimental demonstration of the proposed control method.

For testing purposes, the training grid is selected as a sequence of moves that are intentionally different from the robot moves expected in regular operation (including the two test moves). This is to verify the ability of the neural network to predict modeling errors for any moves within the training grid, which differentiates the NN-based control from the ILC approach.

Fig. 11 shows the tracking errors perpendicular to the path of the active end-effector (normal errors) for an extend and retract motion to/from a typical process station. The thin line shows the tracking performance using the original computed-torque method whereas the bold line represents the neural-network-based approach. Likewise, Fig. 12 shows the comparative results for another station with a different access path elsewhere in the workspace of the robot. The experimental results demonstrate that the neural network-based approach substantially improved the existing computed-torque algorithm. In both cases the tracking errors are at least two times better than the original performance.

Further information on the NN-based perturbation estimation approach, including more details on the control design, training grid and experimental testing, can be found in Moura and Hosek (2003).

6. CONCLUSION

In this study, four advanced control and identification methods were proposed to improve closed-loop stability and tracking performance of substrate-handling robots with undesirable structural flexibilities and frictional effects. The methods included sensorless modal stabilization, observer-corrector control strategy, iterative learning control approach and neural-network-based perturbation estimation. The fundamentals of the methods were outlined, and the effectiveness of each of them was demonstrated experimentally in an industrial application.

REFERENCES

Bien Z. and Xu J. X (1998). *Iterative Learning Control: Analysis, Design, Integration and Applications.* Kluwer Academic Publishers.

Caveney R. T. and Hofmeister C. A. (1998). Robot Handling Apparatus, U.S. Patent No. 5,765,983.

Davis J. C. and Brooks N. B. (1988). Articulated Arm Transfer Device, U.S. Patent No. 4,730,976.

Davis J. C. and Hofmeister C. A. (1997). Substrate Transport Apparatus with Dual Substrate Holders, U.S. Patent No. 5,647,724.

Friedland B. (1996). *Advanced Control System Design,* Section 7.6 - Unmodeled Resonances. Prentice Hall, Englewood Cliffs, New Jersey.

Fu K. S., Gonzales R. C. and Lee C. S. G. (1987). *Robotics: Control, Sensing, Vision, and Intelligence.* McGraw-Hill, New York.

Elmali H. and Olgac N. (1992). Sliding Mode Control with Perturbation Estimation (SMCPE): a New Approach. *International Journal of Control,* **56**, 923-941.

Hendrickson R. A. (1993). Articulated Arm Transfer Device, U.S. Patent No. 5,180,276.

Hosek M. (2001a). Sensorless Modal Stabilization for Three-Link Robotic Arm with Elastic Wrist Drive Belt, 2001 ASME DETC, September 9-12, Pittsburgh, PA.

Hosek M. (2001b). Observer-Corrector Control Strategy for Robotic Manipulators with Unmodeled Dynamics, 2001 ASME IMECE, November 11-16, New York, NY.

Hosek M. and Elmali H. (2001). System of Trajectory Planning for Robotic Manipulators Based on Pre-Defined Time-Optimum Trajectory Shapes, U.S. Patent No. 6,216,058.

Hosek M. and Elmali H. (2003). Trajectory Planning and Motion Control Strategies for a Planar Three-Degree-of-Freedom Robotic Arm, U.S. Patent No. 6,643,563.

Hosek M., Moura J. T. and Elmali H. (2001), Implementation of Observer-Corrector Feedback for Motion Control of Direct-Drive Robotic Manipulator, 2001 ASME IMECE, November 11-16, New York, NY.

Hosek M., Moura J. T. and Elmali H. (2003). Observer-Corrector Control System for Systems with Unmodeled Dynamics, U.S. Patent No. 6,567,711.

Hosek M. and Prochazka J. (2005). On-The-Fly Substrate Eccentricity Recognition for Robotized Manufacturing Systems. *Journal of Manufacturing Science and Engineering,* **127**, 206-216.

Levine W. S. (Ed.) (1996a). *The Control Handbook,* Section 77.3 - Ultra-High Precision Control. CRC Press, Boca Raton, Florida.

Levine W. S. (Ed.) (1996b). *The Control Handbook.* Section 58.2 - General Parameter Estimation Techniques. CRC Press, Boca Raton, Florida.

Moura J. T., Elmali H. and Olgac N. (1997). Sliding Mode Control with Sliding Perturbation Observer. *Journal of Dynamic Systems Measurement and Control,* **119**, 657-665.

Moura J. T. and Hosek M. (2003). Neural Network Based Perturbation Identification Approach for High Accuracy Tracking Control of Robotic Manipulators, 2003 ASME IMECE, November 16-21, Washington, DC.

Press W., Flannery, B., Teulkolsky, S. and Vetterling, W. (1990) *Numerical Recipes in C.* Cambridge Press.

Rojas R. (1996). *Neural Networks – A Systematic Introduction.* Springer-Verlag, Berlin, New York.